Journal of Building Material Science
https://journals.bilpubgroup.com/index.php/jbms

ARTICLE

Washout and Strength Behaviors of Underwater Concrete Containing Welan Gum and Slump Retainers

Joseph Jean Assaad

Department of Civil & Environmental Engineering, Faculty of Engineering, University of Balamand, Koura Campus, Tripoli P.O. Box 100, Lebanon

ABSTRACT

This study explores the synergistic effects of welan gum-based anti-washout admixtures (AWAs) and slump-retaining polycarboxylate ether superplasticizers (SK-PCEs) in underwater concrete (UWC). It addresses the inherent challenge of simultaneously achieving sufficient viscosity to resist washout while maintaining adequate workability for extended placement. Three mortar series incorporating different water-to-binder (w/b) ratios and AWA/SK-PCE combinations were investigated through tests of time-dependent flow behavior, washout resistance, V-funnel flow time, bleeding, setting time, and compressive strength. Test results showed that the incorporation of SK-PCE is efficient to reduce the rate of flow loss over time, yet without altering the V-funnel flow time (i.e., viscosity) measurements. At a high w/b of 0.5, the AWA's ability to trap mixing water (bleeding) and reduce washout loss was slightly disrupted by the SK-PCE. However, at lower w/b of 0.42 and 0.36, the negative SK-PCE impact becomes negligible, suggesting that the inherent particle packing and naturally cohesive mixtures compensate for the dispersive energy provided by the PCE polymers. While the incorporation of AWA prolonged setting and reduced late-age compressive strength, the addition of SK-PCE alongside AWA had a neutral effect. From a practical standpoint, this reflects the possibility of adjusting the AWA and SK-PCE couple in order to optimize washout resistance and workability drop without dramatically compromising the setting and durability of UWC mixtures.

Keywords: Welan Gum; Polycarboxylate Ethers; Underwater Concrete; Washout Loss; Compressive Strength

*CORRESPONDING AUTHOR:
Joseph Jean Assaad, Department of Civil & Environmental Engineering, Faculty of Engineering, University of Balamand, Koura Campus, Tripoli P.O. Box 100, Lebanon; Email: joseph.assaad@balamand.edu.lb

ARTICLE INFO
Received: 18 June 2026 | Revised: 6 July 2026 | Accepted: 16 July 2026 | Published Online: 13 August 2026
DOI: https://doi.org/10.30564/jbms.v8i3.13659

CITATION
Assaad, J.J., 2026. Washout and Strength Behaviors of Underwater Concrete Containing Welan Gum and Slump Retainers. Journal of Building Material Science. 8(3): 105–121. DOI: https://doi.org/10.30564/jbms.v8i3.13659

1. Introduction

The fresh underwater concrete (UWC) properties must be thoroughly tailored to ensure successful construction and repair of marine and hydraulic structures. Unlike conventional concrete cast and consolidated above water, vibration is prohibited for UWC mixtures since this could induce significant cement paste washout and aggregate segregation, which could deteriorate the hardened concrete properties [1,2]. Properly proportioned UWC must exhibit sufficient fluidity to ensure proper self-leveling while maintaining adequate cohesiveness and internal stability to resist washout and bleeding during underwater placement.

Numerous researchers reported that the washout risks significantly increased for UWC mixtures possessing higher workability (i.e., slump flow exceeding about 600 mm) [3,4]. In such situations, the UWC matrix is less cohesive and typically prone to separation during underwater casting, directly impacting the mechanical performance. For instance, Assaad and Issa showed that reducing washout from 13% to 4% led to improved residual compressive strength from 72% to 90% [5]. The strength deficit is primarily driven by three factors, including the physical washout loss of the cementitious phase, disruption of the mixture homogeneity caused by aggregate segregation during discharge, and water infiltration within the plastic concrete until the onset of hardening. The use of high-range water reducers (HRWRs) is essential to secure the high fluidity required for self-consolidation at the point of discharge while maintaining a low water-to-binder ratio (w/b) to safeguard the concrete strength and structural integrity [2].

Antiwashout admixtures (AWAs) are commonly incorporated to reduce the dilution (or, washout) of the cementitious matrix, which enhances the resistance against erosion of exposed surfaces and maintains acceptable residual compressive and bond strengths to reinforcing bars [6,7]. The AWAs, such as cellulose derivatives or microbial polysaccharides like welan gum, function primarily through aqueous phase thickening and inter-particle bridging. The long-chain molecules of the AWA contain numerous hydrophilic groups that adsorb and fix large volumes of water. This increases the viscosity of the pore solution, making it harder for external water to penetrate and dilute the matrix. Zhang et al. [8] reported that AWA polymers develop a three-dimensional network within the paste, acting as a molecular glue to tether the fine particles together and create a thixotropic structure that resists the kinetic energy of water during free-fall or current exposure.

The UWC mix constituents must be thoroughly tailored, since the mechanism that prevents washout (i.e., high plastic viscosity) is the same mechanism that restricts flow. From a rheological point of view, AWAs significantly increase the yield stress (i.e., the force needed to start movement) and plastic viscosity (i.e., the resistance to flow once moving) of cementitious materials [1,9]. Nevertheless, while a high AWA dose may lead to zero washout, the resulting UWC may fail to achieve optimum consolidation around the reinforcement bars or fill the corners of a repair patch, leading to internal voids and honeycombing. Furthermore, it has been shown that AWA polymers often compete with superplasticizers for adsorption onto the cement particles, which can accelerate the loss in workability [10]. It is worth mentioning that the use of set-retarders commonly based on sodium gluconate and glucoheptonate often delay the setting times and early strength development, making them inappropriate for UWC proportioning [11].

Slump-keeping polycarboxylate ethers (SK-PCEs) are designed to prolong the workability window between mixing and placement of fresh concrete [12,13]. This can be particularly useful during hot weather concreting and large-scale construction works requiring several hours of continuous pours. In underwater works involving deep-sea tremie placements or repair of submerged piles, extended workability is critical, since the concrete must often travel through hundreds of meters of tremie piping without clogging. If the workability is reduced during the pouring process, the concrete can plug inside the pipes, with dramatic consequences affecting the equipment functionality and structural integrity due to the formation of cold joints and honeycombing [6]. This can be particularly exacerbated with AWA additions, requiring the use of SK-PCEs.

Unlike conventional PCEs, the SK-PCEs are grafted with functional groups within their polymer chemical structure to exhibit a slower release mechanism that prevents the rapid workability loss and premature stiffening [14,15]. The polymers function by adsorption onto the cement particles, while the grafted side chains are gradually detached under the high alkaline cementitious solution to release the active dispersing segments over time [16,17]. Commonly used side-chains include modified phosphates or cationic monomers of carboxyl and ester groups that prolong the induction period of cement hydration while providing a mild retarding effect [18,19]. Chen et al. [20] reflected the importance of properly balancing the carboxyl and ester groups in order to maximize initial dispersion, while simultaneously securing enough delayed action to improve flowability retention over time. Hence, if the active grafted functional groups are rapidly released, these can be consumed by the cement hydrated compounds, leading to polymer depletion and early stiffening [20]. Simply increasing the superplasticizer dose to mitigate early polymer depletion is not recommended, since this induces a dramatic drop in the yield stress and plastic viscosity with detrimental effects on the UWC washout and segregation phenomena.

Scope and Paper Objectives

The effectiveness of AWAs in reducing the UWC washout loss and the ability of SK-PCEs in improving slump retention have been examined independently [7,21,22]. Consequently, the combined interplay between welan gum AWAs and SK-PCEs remains unexplored, particularly knowing the competing mechanisms of action governing such polymers in the UWC system. The compatibility of these admixtures for mixtures with different water-to-binder ratios (w/b), including their effects on workability, washout, setting, and strength, remain insufficiently understood and require further assessment.

This paper is part of a research program undertaken to (i) evaluate the flow retention of UWC systems incorporating different concentrations of AWA and SK-PCE polymers; (ii) establish the link between washout loss and residual compressive strengths determined in dry and submerged conditions; and (iii) provide practical guidance for dosage optimization in underwater casting applications requiring extended UWC flow retention, yet with controlled influence on setting times and hardened properties. Three concrete-equivalent-mortar mixtures possessing relatively low to high stability levels are evaluated in this study through measurements of time-dependent flow, V-funnel flow time, bleeding, washout loss, setting, and compressive strength. Data presented in this paper can be of particular interest to concrete engineers and consultants involved in underwater construction requiring optimized AWA and SK-PCE additions to improve workability retention without compromising washout resistance or hardened properties.

2. Experimental Program

2.1. Materials

ASTM C150 Type I Portland cement and ASTM C989 Grade 100 ground granulated blast furnace slag were used. The cement had a specific gravity of 3.15 and a Blaine fineness of 325 m^2/kg, while the slag presented a specific gravity of 2.87 and a Blaine fineness of 440 m^2/kg. The cement composition comprised 63.1% C_3S, 6.2% C_3A, and sodium equivalent (Na_2O_{eq}) of 0.55%. The binder consisted of 75% cement and 25% slag. The fine aggregate consisted of ASTM C33 siliceous sand having a 4.75 mm nominal size, a 2.45 fineness modulus, and a 2.65 specific gravity.

A commercially available PCE-based high-range water reducer (HRWR) characterized by its high initial dispersion properties is used to achieve the required flowability. Its specific gravity, pH, and solid content are 1.055, 6.2, and 30.5%, respectively. According to the manufacturer, this HRWR is formulated for rapid adsorption onto cement particles to maximize early dispersion, with a recommended dosage ranging from 0.2% to 1.2%, by mass of binder.

The SK-PCE is used to extend the flowability of tested mixtures. This admixture is designed using anionic functional groups to reduce early adsorption onto cement grains, thus maintaining a greater fraction of dissolved polymers in the pore solution for better flow retention. Its specific gravity, pH, and solid content were 1.052, 6.5, and 30.3%, respectively, while its recommended dosage ranges from 0.1% to 0.8%, by mass of binder.

A powder form of Welan gum (from Kelcocrete) acting as AWA was employed in this study. To ensure uniform dispersion and prevent agglomeration, the powder was pre-dissolved in a portion of the mixing water to create a 5% aqueous solution. This solution was prepared using a high-shear mixer at 500 rpm for 10 min, and subsequently substituted for an equivalent mass of the total mixing water during mortar preparation.

2.2. Mix Proportions

As shown in **Table 1**, three UWC categories are considered in this experimental program with binder contents of 375, 435, and 500 kg/m^3. The w/b varied from 0.50 to 0.42 and 0.36, thus offering a wide range of stability and cohesiveness levels. The sand-to-total aggregate ratio remained constant at 0.45.

The experimental program utilized the concrete-equivalent-mortar (CEM) method for testing the performance interactions between AWA and SK-PCE (**Table 1**). This technique preserves the binder content and w/b of the parent concrete while substituting the coarse aggregates with a quantity of sand having an equivalent specific surface area [4,23]. By minimizing the confounding effects of coarse aggregate internal friction and surface roughness, the CEM approach enables a more precise characterization of the mortar cohesiveness due to admixture additions, including the matrix's proneness to washout loss and drop in compressive strength in humid environments.

Table 1. The UWC mix proportions and corresponding CEM.

	UWC1	**UWC2**	**UWC3**
	Mass (kg/m^3)/Specific Gravity = Volume (L/m^3)		
Binder	375/3.15 = 119.05	435/3.15 = 138.09	500/3.15 = 158.73
Water	187.5	182.7	180
w/b	0.5	0.42	0.36
Sand (0–4.75mm)	800/2.6 = 307.7	780/2.6 = 300	760/2.6 = 292.3
Aggregate (1.18–9.5mm)	960/2.7 = 355.5	950/2.7 = 351.8	920 /2.7 = 340.7
Air content %	3	2.6	2.9
Total volume, L/m^3	999.79	998.64	1000.77
	CEM1	**CEM2**	**CEM3**
Binder, kg/m^3	375	435	500
w/b	0.5	0.42	0.36
Sand (0–4.75mm), kg/m^3	1035	1020	980
AWA, % of binder	0%, 0.15%, or 0.4%	0% or 0.3%	0% or 0.2%
SK-PCE, % of binder	0%, 0.2%, or 0.4%	0%, 0.25%, or 0.5%	0%, 0.3%, or 0.6%
HRWR, % of binder	Various to achieve a fixed initial flow of 220 ± 10 mm		

This experimental program was designed to evaluate the interactions between AWA and SK-PCE across the three distinct stability regimes. Hence, within each category, the following protocol was applied:

- A control mix was prepared, with the HRWR adjusted to achieve a constant initial flow of 230 ± 10 mm, as per ASTM C230. This corresponds to approximately a slump flow diameter of 650 × 650 mm in concrete mixtures, allowing underwater casting to be realized without vibration [1].
- The AWA was then introduced at different dosage rates to reduce washout loss, while again adjusting the HRWR to maintain the same initial flow. As shown in **Table 1**, the AWA varied from 0.15% to 0.4% for mixtures prepared with 0.5 w/b, while this was gradually reduced to 0.3% and 0.2% for mortars made with 0.42 or 0.36 w/b, given the increased cohesiveness due to the reduced free mixing water.
- Given the significant loss in flow encountered following AWA additions, the SK-PCE was introduced at pre-determined rates in order to limit the drop in flow within 160 ± 10 mm during a time interval of 60 min from batching. The 60-minute interval period is considered enough for proper concrete casting during underwater works [1]. Hence, for example, the SK-PCE was introduced at 0.2% or 0.4% in the 0.5-w/b mixtures containing 0.15% or 0.4% AWA, respectively. As earlier, the HRWR was always adjusted to ensure that the initial target flow of 230 ± 10 mm was achieved.

Mixing was conducted in a climate-controlled environment (23 °C, 50% RH). The sand was initially pre-blended with 50% of the mixing water, after which the cementitious materials were introduced over 30 s. The

HRWR was subsequently added along with the remaining water, then the SK-PCE and AWA, followed by 1.5 min of continuous mixing. After a 30-second rest period, the process concluded with a final 1.5-minute mixing cycle to ensure the homogeneity of the mixture.

2.3. Testing Methods

Following the end of mixing, the flow and its evolution during a 60-minute interval period, unit weight, V-funnel flow time, bleeding, washout loss, setting time, and compressive strength are determined. The mini-slump cone measures 70 mm at the top and 100 mm at the bottom, with a total height of 50 mm, as per ASTM C230 specification [24]. Measurements were made right after mixing up to 60 min, at 15-minute time intervals. The mortar was kept in a bowl covered by wet burlap during the rest period, yet vigorously mixed for 5 min prior to each test.

The flowability and relative viscosity were assessed via the V-funnel test, utilizing a modified Marsh cone with a 500 mL capacity and a 12.7 mm discharge orifice [18]. Measurements were made right after the completion of mixing to ensure consistent data. The V-funnel flow was recorded as the time needed for the total mortar discharge, as shown by the first appearance of light through the apparatus orifice.

Bleeding was determined as per ASTM C232 using 75 × 150 mm cylinders [25]. The bleed water was periodically collected from the mortar's surface using a pipette and weighed to the nearest 0.01 g. The bleeding capacity was calculated as the ratio of the total decanted water mass to the mass of mixing water present in the sample, expressed as a percentage. This test is critical for assessing the stability of UWC mixtures across the varying w/b values. Replicate values are considered for the V-funnel and bleed water tests.

Figure 1 shows the experimental set-up adapted from the CRD C61 test method to evaluate the washout loss of CEM mixtures without coarse aggregates [4,26]. Approximately 1 kg of fresh mortar was placed in a wire-mesh basket and subjected to a free-fall drop through a 1 m water column. The basket dimensions adhered to the original CRD C61 specifications, with 1.5 mm nominal diameter of the circular perforations to minimize material loss during the initial filling process. Following a 15 s immersion period at the column base, the basket is retrieved at a constant velocity of 0.5 m/s and weighed. The washout loss, designated as W, is determined based on a single drop cycle; the average of three measurements is taken. Testing was done right after mixing (referred to as W_0) as well as after the conclusion of each flow test realized throughout the 60-minute time interval. For example, W_{30} and W_{60} refer to washout loss determined after 30 or 60 min, respectively. Just like the flow test, the mortar specimen was kept in the bowl covered by a wet burlap during the rest period, and vigorously mixed for 5 min prior to washout testing.

Initial and final setting times were evaluated using the penetration resistance method (ASTM C403) [27]. Samples were maintained under controlled laboratory conditions to eliminate the influence of humidity and temperature fluctuations. The setting times were determined by identifying the points at which the penetration resistance reached the 3.5 MPa (initial) and 27.6 MPa (final) thresholds, allowing for an assessment of the impact of admixture combinations on cement hydration kinetics.

The compressive strength was evaluated in accordance with ASTM C109 under both dry and submerged casting conditions [28]. For the submerged specimens, two distinct casting methods were employed:

- Method 1 (Re-homogenized): Mortar samples previously subjected to the washout test were manually homogenized in a bowl and subsequently cast into 50 mm cube molds. This approach has been validated in prior studies to correlate effectively with the UWC mechanical properties, including the bond strength to reinforcing bars [6].
- Method 2 (Underwater gravity casting): Molds are placed in a reservoir filled flush with water. The freshly mixed mortar was poured without any consolidation using a modified Marsh cone positioned 10 mm above the water surface. This method has proven effective in predicting the impact of washout loss on the residual pull-off bond strength of underwater geopolymer repairs [29].

Regardless of the casting condition, all specimens were demolded after 24 h and cured in lime-saturated water at 20 ± 3 °C. Compressive strength results at 28 days are reported as the average of three replicate specimens.

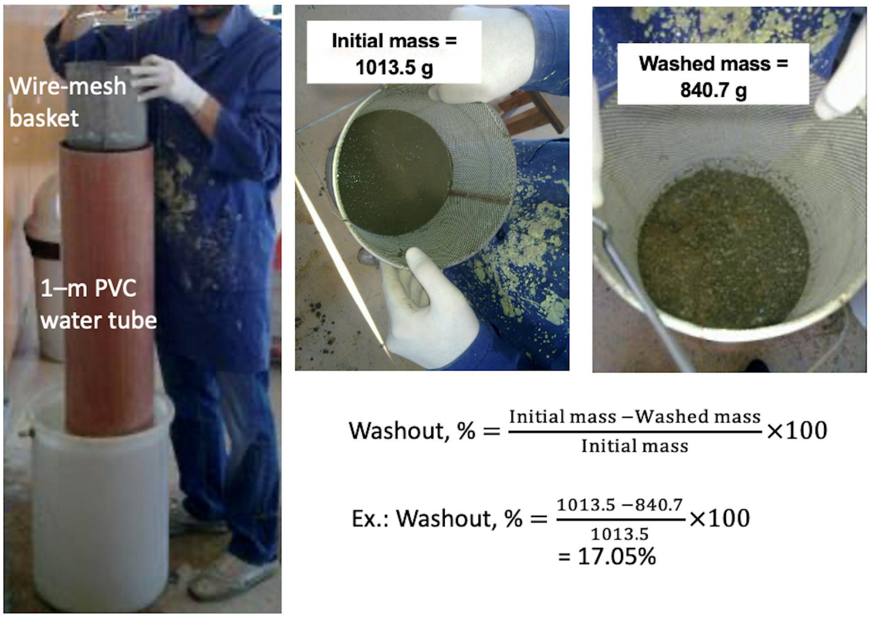

Figure 1. Photo of the washout set-up test.

3. Test Results and Discussion

3.1. HRWR Demand

The HRWR dosages required to ensure an initial flow of 230 ± 15 mm for tested mortars are summarized in **Table 2**, along with the variations in flow during the 60-minute interval period. As expected, the incorporation of AWA increased the HRWR demand, primarily due to competitive adsorption and increased viscosity [30–32]. For example, the HRWR increased from 0.45% for the 0.5-w/b control mix to 0.66% and 1.05% for mortars incorporating 0.15% or 0.4% AWA, respectively. Earlier studies showed that the large AWA polymer chains (including welan gum) can physically wrap around the cement particles and interfere with the combs of PCE molecules, reducing their thinning efficiency [20]. Concurrently, the AWAs bind portions of the free mixing water into a three-dimensional gel network, leading to increased viscosity and internal friction, which necessitate higher HRWR dosage. As shown in **Table 2**, the addition of SK-PCE seems to exhibit a negligible influence on the HRWR demand, hinting at its limited contribution to the initial dispersion of the cement grains.

Table 2. HRWR demand and flow variations over time for tested mixtures.

	HRWR, %	AWA, %	SK-PCE, %	Flow (mm) after Various Rest Intervals of t_0, t_{15}, t_{30}, t_{45}, and t_{60}, Respectively	Rate of Flow Loss, mm/min
0.5w/b	0.45	0	0	230, 190, 175, 145, 125	−1.7
0.5w/b–0.15AWA	0.66	0.15	0	225, 180, 150, 110, n/a	−2.5
0.5w/b–0.4AWA	1.05	0.4	0	230, 155, 110, n/a, n/a	−4
0.5w/b–0.15AWA–0.2SK	0.65	0.15	0.2	235, 205, 190, 175, 160	−1.2
0.5w/b–0.4AWA–0.4SK	1.02	0.4	0.4	225, 205, 195, 180, 165	−0.97
0.42w/b	0.66	0	0	235, 200, 170, 150, 120	−1.87
0.42w/b–0.3AWA	0.85	0.3	0	225, 170, 130, n/a, n/a	−3.17
0.42w/b–0.3AWA–0.25SK	0.85	0.3	0.25	230, 195, 180, 165, 140	−1.4
0.42w/b–0.3AWA–0.5SK	0.8	0.3	0.5	230, 205, 195, 190, 170	−0.9
0.36w/b	1.05	0	0	225, 180, 155, 130, n/a	−2.07
0.36w/b–0.2AWA	1.32	0.2	0	230, 175, 140, 110, n/a	−2.63
0.36w/b–0.2AWA–0.3SK	1.32	0.2	0.3	235, 205, 190, 170, 150	−1.37
0.36w/b–0.2AWA–0.6SK	1.3	0.2	0.6	230, 210, 195, 180, 170	−1

3.2. Time-Dependent Flow Variations

Figure 2 presents the evolution of flow over time for mortars prepared with 0.5 w/b. While the control mix exhibited a moderate flow loss rate of −1.7 mm/min, the incorporation of AWA yielded significantly sharper declines driven by a combination of water immobilization and the formation of a polymeric structural network [9]. The corresponding flow loss rate increased to −2.5 and −4 mm/min at AWA dosage of 0.15% or 0.4%, respectively. The former phenomenon (i.e., water immobilization) is typically ascribed to the long-chain hydrophilic microbial gums that soak up and chemically bind a significant portion of the free mixing water, leading to higher internal friction and immediate flow loss. On the other hand, the dissolved AWA polymer chains overlap and tangle, creating a microscopic mesh throughout the matrix that increases the resistance to flow.

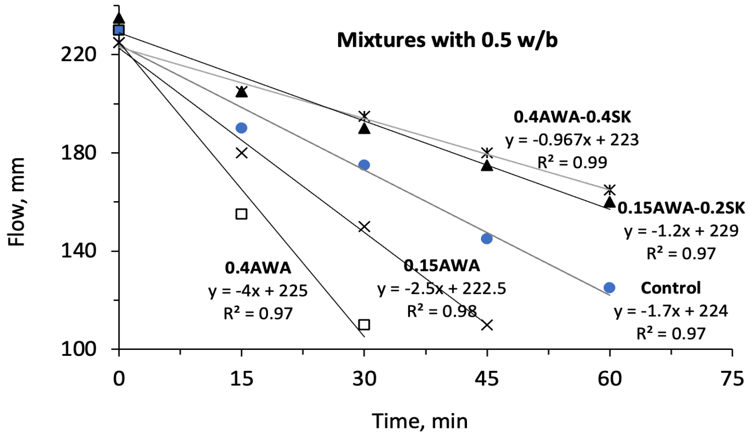

Figure 2. Typical flow variations over time for 0.5-w/b mixtures.

As shown in **Figure 2**, the slopes flattened remarkably when the SK-PCE was coupled with AWA, with the flow values remaining larger than 160 mm after 60 min. Hence, the resulting flow loss rate dropped to −1.2 and −0.967 mm/min for the 0.15AWA–0.2SK and 0.4AWA–0.4SK mixtures, respectively. This can be attributed to the time-dependent activation of the PCE functional groups [14], trying to slide within the AWA polymeric networks to keep the system moving. The higher AWA dose at a given w/b requires more functional groups to maintain the flow. Chen et al. [20] reported that the gradual alkaline hydrolysis of ester groups caused the additional carboxylates to be slowly released into the pore solution over time, supplementing the initially adsorbed polymer fraction. In other words, this suggests the presence of a clear synergistic effect between AWA and SK-PCE in UWC mixtures; while AWA provides the necessary stability (washout resistance), SK-PCE provides the time-release fluidity needed to maintain proper workability over time.

Regardless of w/b, the flow loss rate varied within a narrow range (i.e., between −0.9 and −1.4 mm/min) for mixtures containing the couple AWA and SK-PCE polymers (**Table 2**). This confirms that the sacrificial time-release mechanism of the SK-PCE successfully balanced the AWA-induced thickening across the different mix designs with varying water contents. From a practical standpoint, it is worth noting that a flow reduction from an initial value of 230 mm (equivalent to 650 × 650 mm concrete slump flow) to approximately 160 mm (equivalent to 350 × 350 mm slump flow) within 60 min is considered acceptable. This allows engineers to effectively manage workability and predict underwater casting behavior during construction [1].

3.3. V-Funnel Flow and Bleeding

Table 3 summarizes the unit weights, V-funnel flow times, and bleeding characteristics (i.e., maximum value, and its rate of increase determined during the first 10-minute), washout loss, and setting times. The table also includes for the 0.42-w/b mixture series the coefficients of variation (COV) determined as the ratios of the mean value divided by the standard deviation, multiplied by 100. Generally speaking, the COVs were pretty limited for the V-funnel and bleeding tests (i.e., less than 4.4%). The COV varied between 6.2% and 8.8% for the washout loss determined after mixing, and then increased to 9.1% and 12% at the end of the flow test.

Table 3. Fresh properties, washout loss, and setting times for tested mixtures.

	Unit Weight, kg/m³	V-Funnel, sec	Bleeding		Washout loss, %		Set Time, hr:min
			Max. Value, %	Rate, %/min	Initial W_0	W at End of Flow Test	
0.5w/b	1,905	29.5	9.7	0.90	17.2	W_{60} = 8.1	9:10
0.5w/b–0.15AWA	1,910	43	4.6	0.39	12.1	W_{45} = 6	10:45
0.5w/b–0.4AWA	1,885	75	2.3	0.17	4.2	W_{30} = 1.7	13:20
0.5w/b–0.15AWA–0.2SK	1,910	46.5	5.2	0.44	10.6	W_{60} = 8.4	11:05
0.5w/b–0.4AWA–0.4SK	1,900	68	4	0.36	4.8	W_{60} = 3.1	13:40
0.42w/b	1,975 (2.1%)	42 (3.4%)	4.8 (3%)	0.40	13.1 (6.2%)	W_{60} = 5.9 (10.3%)	8:05 (5.3%)
0.42w/b–0.3AWA	1,950 (2%)	70.5 (3%)	2.5 (2.3%)	0.19	4.2 (8.8%)	W_{30} = 1.9 (12%)	10:10 (6%)
0.42w/b–0.3AWA–0.25SK	1,960 (1.8%)	68 (3.8%)	3.1 (3.4%)	0.23	3.5 (8%)	W_{60} = 2.2 (9.1%)	10:05 (7.4%)
0.42w/b–0.3AWA–0.5SK	1,960 (2.3%)	72 (3.9%)	3.0 (4.4%)	0.25	4.2 (7.5%)	W_{60} = 3 (10.1%)	10:45 (6.7%)
0.36w/b	2,040	61	3.1	0.28	8.8	W_{45} = 3.8	7:50
0.36w/b–0.2AWA	2,015	82.5	1.8	0.12	3.6	W_{45} = 1.9	9:10
0.36w/b–0.2AWA–0.3SK	2,010	88	2.4	0.21	3.2	W_{60} = 2.3	9:35
0.36w/b–0.2AWA–0.6SK	2,020	85.5	2.2	0.21	3.4	W_{60} = 2.9	9:30

Because of water immobilization and the formation of polymeric networks, the incorporation of AWA remarkably improved the mortar stability, leading to increased V-funnel flow time and reduced bleeding. For example, the flow time increased from 29.5 s for the control 0.5-w/b mix to 43 and 75 s when 0.15% or 0.4% AWA was added, respectively. The corresponding bleeding dropped from 9.7% to 4.6% and 2.3%, respectively, while its rate decreased from 0.9 to 0.39 and 0.17 %/min, respectively. As expected, lowering the free mixing water (i.e., w/b) naturally enhanced internal friction and stability, leading to increased V-funnel flow time and reduced bleeding (**Table 3**).

The overall viscosity remained practically unchanged when the SK-PCE and AWA are both combined in the same mix. For example, the V-funnel flow times varied within a narrow range (i.e., 68 to 72 s) for mixtures prepared with 0.42-w/b. In contrast, however, the interaction of SK-PCE with AWA seems to create a competitive balance within the mortar matrix, which disrupted the AWA's ability to trap water. For example, the rate of bleeding increased from 0.19 %/min for the 0.42w/b-0.3AWA mix to 0.23 and 0.25 %/min when the SK-PCE was added at 0.25% or 0.5%, respectively. This can be attributed to a combination of phenomena, including the high affinity of SK-PCE molecules, which increases adsorption onto cement surfaces, reducing the AWA efficiency to form continuous water-locking films. If the AWA dosage isn't high enough to bridge the newly dispersed particles, free water can migrate to the surface as bleed water. Simultaneously, the SK-PCE involves a slow-release mechanism of polymers that keeps the mortar in a fluid state for a longer period, giving water more time to rise before the restructuring of the matrix.

Strong relationships with correlation coefficients (R^2) larger than 0.9 can be established between the V-funnel flow times and bleeding characteristics, as expressed in Equations (1) and (2):

$$\text{Max. bleeding, \%} = 713.89\ (\text{V-funnel, sec})^{-1.3},\quad R^2 = 0.93, \tag{1}$$

$$\text{Rate of bleeding, \%/min} = 85.57\ (\text{V-funnel, sec})^{-1.39},\quad R^2 = 0.9. \tag{2}$$

Figure 3 illustrates the correlation between the rate of flow loss and the two critical performance indicators, including V-funnel flow time (cohesiveness) and bleeding (stability). For the control and AWA-only mortars, a clear fluidity and performance trade-off is observed. These mixtures followed polynomial trends with R^2 larger than 0.64, where increased V-funnel flow times and/or decreased bleeding are coupled with higher workability loss over time. This suggests that in conventional systems (i.e., without SK-PCE), the physical and chemical mechanisms controlling the initial fluidity are consumed quickly, leading to a predictable but steep degradation in cohesiveness and stability.

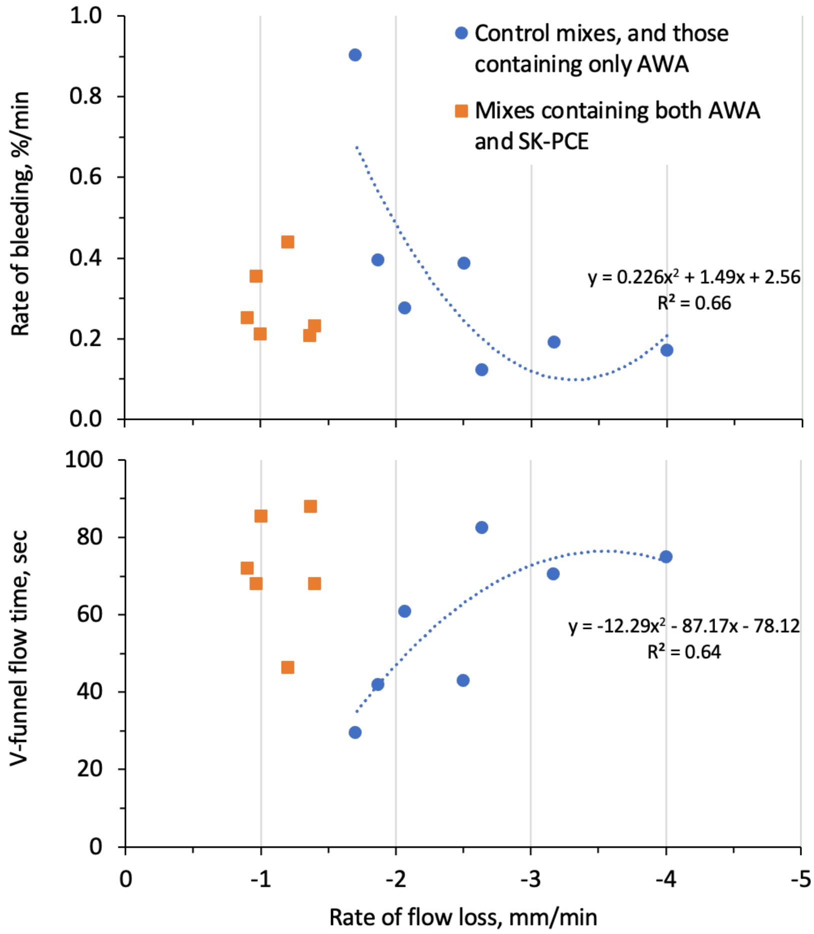

Figure 3. Relationships between the rate of flow loss with respect to the V-funnel flow time and bleeding.

As shown in **Figure 3**, the introduction of SK-PCE fundamentally alters such relationships, which shifted the performance envelope of the produced mortars. The clustering of the orange data points along the left side of the "Rate of Flow Loss" axis reflects the decoupling of the initial workability from its rate of loss. In other words, the SK-PCE maintained consistent lubricating films through controlled polymer release over time, allowing the mortar to remain workable for longer periods. The data points show that the SK-PCE enables the mix to maintain a high level of cohesiveness (V-funnel times between 45–90 s) without the typical penalty of rapid stiffening. From a stability perspective, although the bleeding rate is slightly higher than AWA-only mixes, it remains within a manageable range (i.e., within 0.2–0.45 %/min) for high-performance underwater applications. In other words, the SK-PCE acts as a rheology stabilizer, balancing the viscosity-building network of the AWA to resist washout and segregation while ensuring the adequate maintenance of fluidity to ensure the ease of pumping and placement over extended durations.

3.4. Washout Loss

The results illustrated in **Figure 4** highlight the dominant role of AWA for controlling washout loss, as a result of the formation of a robust polymeric network that increases the pore water viscosity and binds the cementitious particles together [32,33]. Hence, across all w/b series, the inclusion of AWA drastically improved stability; for instance, at 0.5 w/b, the increased AWA dosage from 0% to 0.4% reduced W_0 from approximately 17% to 4%. Over time, the W for the control mix dropped from 8.1% after 60 min to 1.7% for the 0.4 AWA mix after 30 min, underscoring the rapid flow loss and quick restructuring provided by the AWA. Nevertheless, it is worth noting that the main limitation of such data is that the controlled experimental conditions cannot fully replicate complex underwater construction environments, which limits direct field generalization and highlights the need for large-scale or in-situ validation studies.

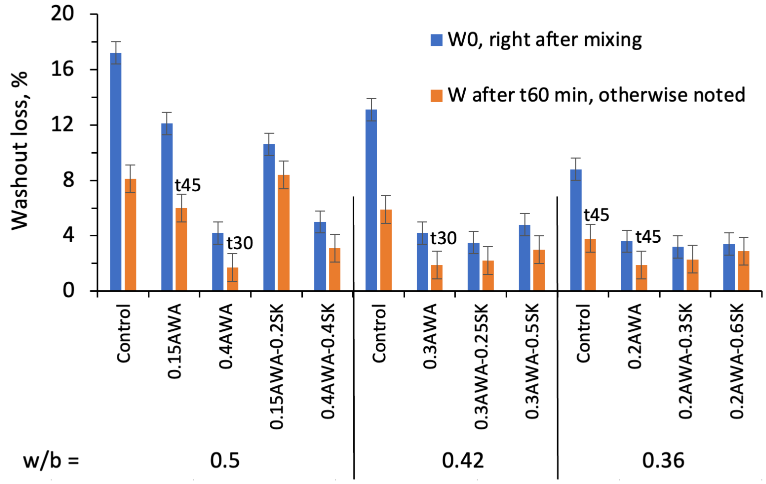

Figure 4. The washout values for all tested CEM mixtures.

The introduction of SK-PCE alongside AWA yielded varying washout effects, mainly depending on w/b. Hence, in the 0.5-w/b series, the addition of SK-PCE (0.4AWA–0.4SK) led to a noticeable increase in washout compared to the AWA-only counterpart (i.e., W_0 increased from 4.2% to 5%), which is likely due to the superplasticizer's ability to compete with the AWA polymers and partially disrupt their protective structure [21,34]. Interestingly, this instability persisted over time; the 0.4AWA–0.4SK mix exhibited a W_{60} of 3.1% after 60 min, as compared to 1.7% for the 0.4AWA mix after 30 min. This suggests that the slump-keeping mechanism that prevents particle flocculation simultaneously delays the formation of a cohesive and washout-resistant matrix skeleton.

Conversely, at lower w/b of 0.42 and 0.36, the negative impact of SK-PCE was negligible, with washout values remaining practically stable and within the repeatability of testing. For example, W_0 varied within a limited range (i.e., from 3.2% to 3.6%) for mixtures prepared with 0.36 w/b and containing AWA alongside SK-PCE. This suggests that in lower w/b systems, the inherent particle packing and naturally cohesive mixture compensate for the dispersive energy provided by the SK-PCE. This, in other words, allows for enhanced flow retention without compromising the anti-washout characteristics required for underwater placement. It is to be noted that adequate relationships exist between W_0 with respect to the V-funnel flow time and bleeding, as plotted in **Figure 5**.

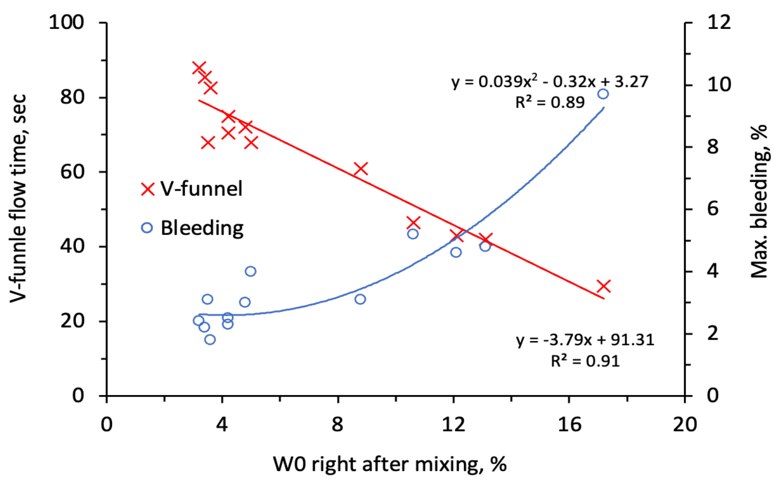

Figure 5. Relationships between W_0 with respect to the V-funnel flow time and bleeding.

Figure 6 illustrates the relationship between the rate of flow loss and the difference between W_0 and the washout value measured over time for the investigated mixtures. A clear performance gap is observed between the control/AWA-only mixes and those modified with the SK-PCE. Hence, the former category of mixtures (blue dots) exhibiting higher and more variable rates of flow loss ranging from −1.8 to −4.0 mm/min are associated with gradually reduced washout values. The resulting R^2 is 0.81. In contrast, the incorporation of SK-PCE (orange squares) shifts the performance into a highly stable zone. Those later mixtures exhibited negligible difference between W_0 and W, which is consistently smaller than 2%, while the flow loss rate was simultaneously restricted to a narrow range varying between −0.9 and −1.4 mm/min. This confirms that the tailored molecular structure of the SK-PCE effectively sustains workability over time, without compromising the cohesive properties required for underwater applications.

3.5. Setting Time

Figure 7 presents the initial setting times of the tested mortars. As shown, the incorporation of AWA remarkably prolonged setting; for example, at a w/b of 0.5, this increased from 9:10 hr:min for the control mix to 10:45 and 13:20 hr:min when 0.15% and 0.4% AWA is added, respectively. The observed retardation is attributed to the steric hindrance and adsorption characteristics of the AWA [14,35,36]. By forming a protective film on the cement grains, the AWA creates a physical barrier that prevents water and ions from reaching the particle surface, slowing down the initial chemical reactions. Concurrently, the AWA thickens the pore water between cement grains and limits the ionic mobility, which slows down the movement (diffusion) of ions and delays the nucleation of hydration products.

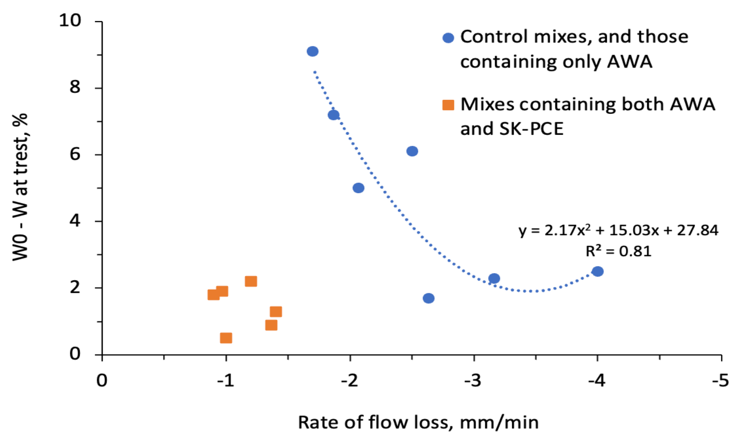

Figure 6. Relationships between the rate of flow loss vs. the difference of washout over time.

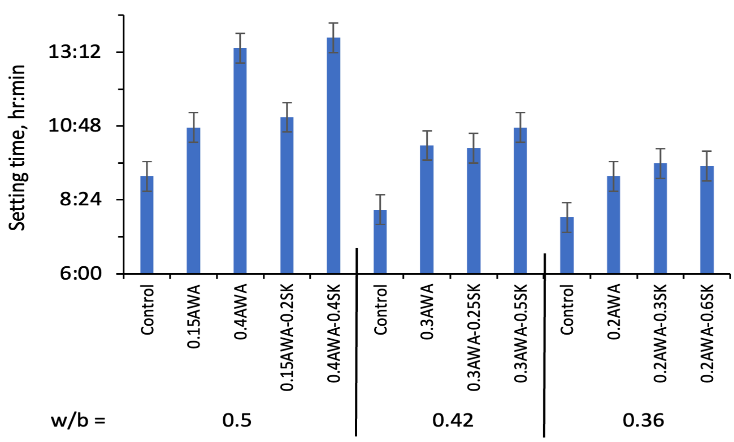

Figure 7. Initial setting times for tested mixtures.

Compared to mixtures containing only AWA, the incorporation of SK-PCE at any given w/b had a negligible influence on setting; the resulting values remained within the repeatability of responses (**Figure 7**). Practically, such results highlight the relevance of properly adjusting the AWA and SK-PCE dosages in order to control the loss in workability without dramatically compromising the setting times of UWC mixtures.

3.6. Compressive Strengths

Table 4 summarizes the 28-day compressive strengths determined in dry or wet condition following the re-homogenizing method of the washed samples or underwater casting in the molds.

Table 4. The 28-day compressive strengths were determined in dry or wet conditions.

	Strength in Dry Condition, MPa	Re-Homogenizing Method		Underwater Gravity Casting	
		Strength in Wet Condition, MPa	Residual Strength, %	Strength in Wet Condition, MPa	Residual Strength, %
0.5w/b	30.7	21.3	69.38	18	58.63
0.5w/b–0.15AWA	28.8	24.7	85.76	22.5	78.13
0.5w/b–0.4AWA	25.6	24.2	94.53	23.2	90.63
0.5w/b–0.15AWA–0.2SK	28.2	23.9	84.75	23.6	83.69
0.5w/b–0.4AWA–0.4SK	25	23.1	92.40	23	92.00
0.42w/b	41.6	32.4	77.88	31.2	75.00
0.42w/b–0.3AWA	36.7	34	92.64	31.1	84.74
0.42w/b–0.3AWA–0.25SK	35.5	32.6	91.83	33	92.96
0.42w/b–0.3AWA–0.5SK	36.2	33	91.16	31.4	86.74
0.36w/b	48.7	39.9	81.93	36.3	74.54
0.36w/b–0.2AWA	45	42	93.33	41	91.11
0.36w/b–0.2AWA–0.3SK	44.2	40	90.50	42.8	96.83
0.36w/b–0.2AWA–0.6SK	44.7	39.7	88.81	37.6	84.12

Figure 8 illustrates the values determined in the dry condition, along with the residual strengths determined as 100 minus the ratio between the dry-to-wet strength, divided by the dry strength value. As expected, the compressive strengths determined in the dry condition underscore the classic inverse relationship between w/b and mechanical performance. Yet, in every single w/b category, the addition of AWA led to reduced strength; for example, this dropped from 30.7 MPa for the control 0.5-w/b mix to 28.8 and 25.6 MPa when 0.15% or 0.4% AWA was added, respectively. This can be attributed to the high-molecular-weight AWA polymers that can interfere with the formation of the cement's crystalline structure, like the C-S-H gel [14,16,37]. Pan et al. [10] reported that AWAs can also trap small amounts of extra air during mixing, which creates micro-voids that lower strength. On the other hand, the addition of the SK-PCE had a stabilizing effect on strength, with the resulting values varying within the repeatability of responses (**Figure 8**). This reflects the neutral influence of SK-PCE polymers on the setting times or long-term mechanical performance of UWC mixtures.

The residual strength index serves as a proxy for the washout resistance and underwater integrity of UWC mixtures. Hence, the control mixes across all w/b ratios exhibited significant strength loss (i.e., 25% to 40%) when cast underwater due to severe washout of cement pastes and water infiltration within their skeleton [6]. In contrast, the introduction of AWA drastically altered the mortar's cohesion, yielding increased residual strengths that ranged between 80% and 95%. This corroborates the benefits of combining both admixtures (i.e., AWA and SK-PCE) in the same mixture; while the AWA reduces washout loss and drop in strength, the SK-PCE is incorporated to ensure proper workability retention without compromising the cement hydration kinetics necessary for strength development.

Figure 9 plots the relationships between washout loss determined right after mixing (i.e., W_0) with respect to the residual compressive strengths evaluated following the two distinct casting methods. Both datasets exhibited a strong negative linear correlation, indicating that increased W_0 directly degrades the residual strength of the material, albeit the sensitivity to washout differs significantly between the two methods. Hence, the underwater gravity casting method shows a steeper decline in performance; i.e., for every 1% increase in washout, the material loses nearly 2% of its residual strength. The re-homogenized samples showed a higher R^2 of 0.85, suggesting that the re-homogenization method mitigates some of the structural damage caused by washout loss.

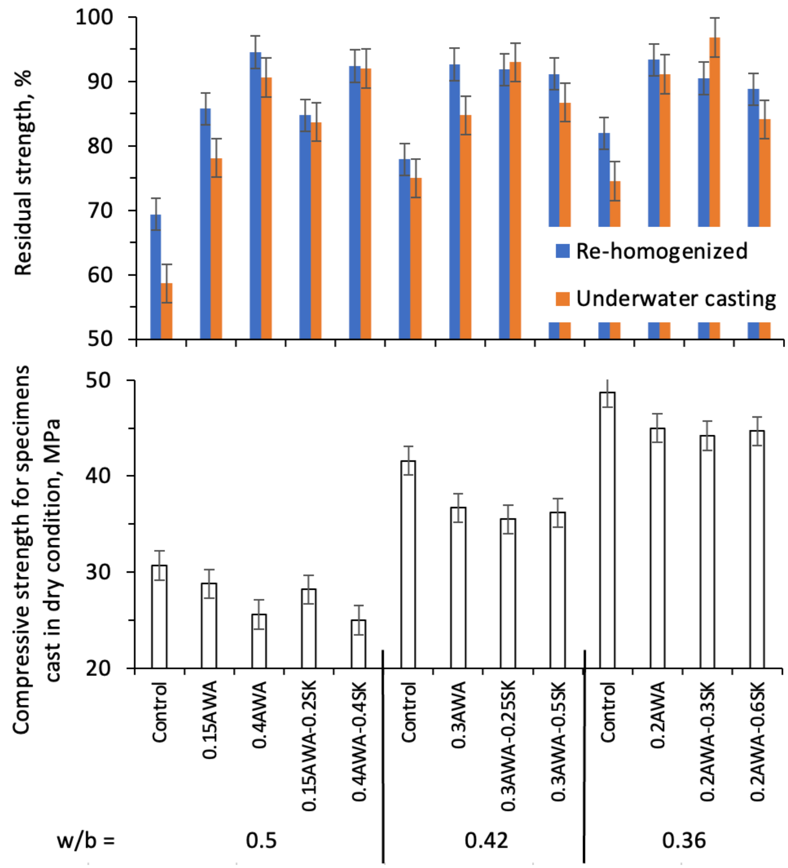

Figure 8. The compressive strengths determined in dry conditions, along with the residual values following casting in wet conditions.

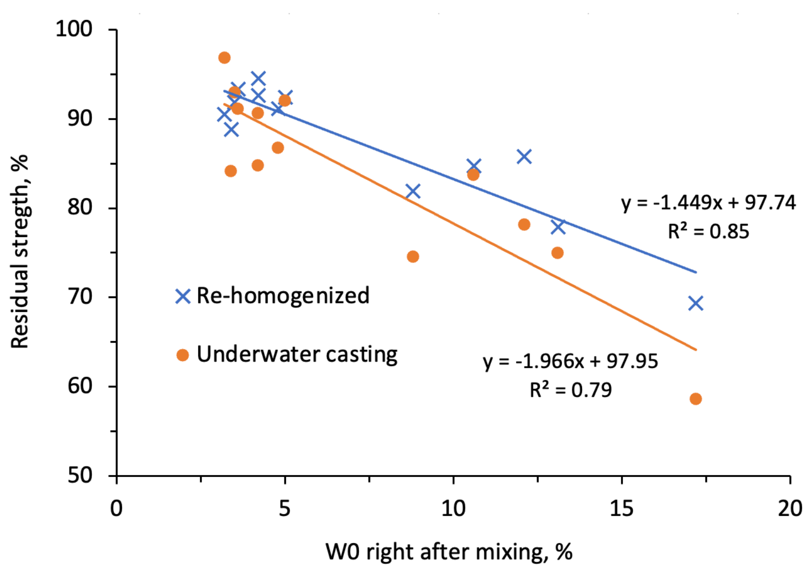

Figure 9. Relationships between W_0 vs. residual compressive strengths evaluated following the two distinct casting methods.

4. Concluding Remarks

This paper explores the synergistic effects of welan gum AWA and SK-PCEs in UWC mixtures. Its main limitation is that the controlled experimental conditions cannot fully replicate the complex underwater construction environments, which highlights the need for large-scale or in-situ validation studies. Future research should include large-scale validation studies and constructability assessments to verify the practical applicability of the proposed mixtures. Additionally, it is important to mention that the mechanisms affecting the cement hydration reactions, setting, and strength development are not directly verified within the scope of this study; rather, these were inferred from the observed macroscopic behavior and supported by findings reported in the literature. While this constitutes a limitation in this study, future work shall include complementary microstructural and chemical characterization techniques (e.g., SEM, EDS, FTIR, XRD, or adsorption analyses) to validate the underlying mechanisms. Based on the foregoing, the following conclusions can be warranted:

1. The rate of flow loss over time significantly increased with AWA additions, due to a combination of water immobilization and the formation of a polymeric structural network. Yet, the rates flattened remarkably when the SK-PCE was added. This suggests the presence of a synergistic effect between AWA and SK-PCE; while AWA provides the necessary stability (washout resistance), SK-PCE provides the fluidity retention needed for proper casting.
2. The V-funnel flow time (viscosity) remained practically unchanged when the SK-PCE and AWA were both combined in the same mix. However, the bleeding characteristics seem to slightly degrade when the SK-PCE is introduced, reflecting the disrupted ability of the AWA to bridge the dispersed cement particles and trap mixing water. The SK-PCE involves a slow-release mechanism of polymers that keeps the mortar in a fluid state for a longer period, giving water more time to rise before the restructuring of the matrix.
3. Mixtures containing AWA and SK-PCE exhibited high cohesiveness levels (V-funnel times between 45–90 s), yet slightly higher bleeding characteristics. This suggests that the SK-PCE acts as a rheology stabilizer for underwater casting, balancing the increased viscosity to resist washout while remaining fluid enough to ensure the ease of pumping and placement over extended durations.
4. Regardless of w/b, the inclusion of AWA drastically improved stability and washout resistance. In contrast, the introduction of SK-PCE alongside AWA yielded varying washout effects, depending on w/b. Hence, in the higher 0.5-w/b series, the addition of SK-PCE led to a noticeable increase in washout compared to the AWA-only counterpart. Conversely, at lower w/b of 0.42 and 0.36, the negative impact of SK-PCE becomes negligible, suggesting that the inherent particle packing and naturally cohesive mixture compensate for the dispersive energy provided by the PCE polymers.
5. The control/AWA-only mixes exhibited gradually reduced washout values at higher rates of flow loss ranging from −1.8 to −4.0 mm/min. Yet, the incorporation of SK-PCE shifts the performance into a stable zone, with the variations in washout being consistently smaller than 2%, and the flow loss rate is restricted within a narrow range between −0.9 and −1.4 mm/min.
6. The incorporation of AWA remarkably prolonged setting and reduced late-age compressive strength. The addition of SK-PCE alongside AWA had a neutral effect, with the responses varying within the repeatability of test results. This highlights the relevance of properly adjusting this couple in order to control washout loss and drop in workability without compromising the setting times and durability of concrete mixtures.
7. Negative linear correlations exist between W_0 and residual strength determined from re-homogenizing the washed samples or underwater gravity casting. The underwater casting method showed a steeper decline in performance, while the re-homogenized samples showed a stronger correlation with R^2 of 0.85.

Funding

This work received no external funding.

Institutional Review Board Statement

Not applicable.

Informed Consent Statement

Not applicable.

Data Availability Statement

The data that support the findings of this study are available from the corresponding author, upon reasonable request.

Conflicts of Interest

The author declares that there is no conflict of interest regarding the publication of this paper.

AI Use Statement

The author declares that no artificial intelligence (AI) tools were used in the preparation of this manuscript.

References

[1] ACI Committee 546, 2010. 546.2R-10: Guide to Underwater Repair of Concrete. American Concrete Institute: Farmington Hills, MI, USA. DOI: https://doi.org/10.14359/51663806

[2] Wang, Y., Chen, S., Qiu, L., et al., 2023. Experimental study on the slump-flow underwater for anti-washout concrete. Construction and Building Materials. 365, 130026. DOI: https://doi.org/10.1016/j.conbuildmat.2022.130026

[3] Horszczaruk, E., Brzozowski, P., 2014. Bond strength of underwater repair concretes under hydrostatic pressure. Construction and Building Materials. 72, 167–173. DOI: https://doi.org/10.1016/j.conbuildmat.2014.08.020

[4] Assaad, J.J., Daou, Y., Harb, J., 2011. Use of CEM Approach to Develop and Optimize High-Performance Underwater Concrete. Journal of Materials in Civil Engineering. 23(7), 1094–1102. DOI: https://doi.org/10.1061/(ASCE)MT.1943-5533.0000254

[5] Assaad, J.J., Issa, C.A., 2013. Mechanisms of strength loss in underwater concrete. Materials and Structures. 46(10), 1613–1629. DOI: https://doi.org/10.1617/s11527-012-0004-2

[6] Issa, C.A., Assaad, J.J., 2015. Bond of tension bars in underwater concrete: effect of bar diameter and cover. Materials and Structures. 48(11), 3457–3471. DOI: https://doi.org/10.1617/s11527-014-0414-4

[7] Yan, W., Cui, W., Qi, L., 2022. Simulation of underwater concrete movement in flowing water using DEM-CFD coupling method. Construction and Building Materials. 319, 126134. DOI: https://doi.org/10.1016/j.conbuildmat.2021.126134

[8] Zhang, Y., Zhao, Q., Liu, C., et al., 2016. Properties comparison of mortars with welan gum or cellulose ether. Construction and Building Materials. 102, 648–653. DOI: https://doi.org/10.1016/j.conbuildmat.2015.10.116

[9] Sun, Z., Xu, B., Yang, Z., et al., 2025. Resolving rheological dilemma in non-dispersible underwater concrete: Conflict between fluidity and anti-washout. Construction and Building Materials. 493, 143258. DOI: https://doi.org/10.1016/j.conbuildmat.2025.143258

[10] Pan, Y., Lu, Z., Li, X., et al., 2026. Enhanced flowability of metakaolin-blended cement through the synergistic effect of polycarboxylate superplasticizer and retarder: Competitive adsorption and retarded hydration. Cement and Concrete Research. 202, 108142. DOI: https://doi.org/10.1016/j.cemconres.2026.108142

[11] Luo, G., Liu, M., Li, H., et al., 2024. Importance of adsorption compared with complexation for retarding C3S hydration via adding sodium gluconate. Cement and Concrete Research. 186, 107686. DOI: https://doi.org/10.1016/j.cemconres.2024.107686

[12] Li, S., Pang, H., Zhang, J., et al., 2019. Synthesis and performance of a novel amphoteric polycarboxylate superplasticizer with hydrolysable ester group. Colloids and Surfaces A: Physicochemical and Engineering Aspects. 564, 78–88. DOI: https://doi.org/10.1016/j.colsurfa.2018.11.043

[13] Liu, X., Guan, J., Lai, G., et al., 2017. Performances and working mechanism of a novel polycarboxylate superplasticizer synthesized through changing molecular topological structure. Journal of Colloid and Interface Science. 504, 12–24. DOI: https://doi.

org/10.1016/j.jcis.2017.05.025
[14] Ma, R., Wang, Y., Li, H., et al., 2023. Progress in the polycarboxylate superplasticizer and their structure-activity relationship – A review. Materials Today Communications. 35, 105838. DOI: https://doi.org/10.1016/j.mtcomm.2023.105838
[15] Lai, G., Liu, X., Song, X., et al., 2024. A mechanistic study on the effectiveness of star-like and comb-like polycarboxylate superplasticizers in cement pastes. Cement and Concrete Research. 175, 107389. DOI: https://doi.org/10.1016/j.cemconres.2023.107389
[16] Li, W., Tan, S., 2026. Effect of functional groups on the dispersion behavior and stability of polycarboxylate superplasticizers in calcium sulfate hemihydrate systems. Materials Letters. 413, 140439. DOI: https://doi.org/10.1016/j.matlet.2026.140439
[17] Pei, J., Li, J., Lv, X., et al., 2026. Synthesis of an early-age strength polycarboxylate lanthanum complex superplasticizer and its impact on cement hydration. Construction and Building Materials. 518, 145820. DOI: https://doi.org/10.1016/j.conbuildmat.2026.145820
[18] Burhan, L., Ghafor, K., Mohammed, A., 2020. Testing and Evaluation of Flowability, Viscosity and Long-Term Compressive Strength of Cement Modified with Polymeric Admixture WR Superplasticizer. IOP Conference Series: Materials Science and Engineering. 737(1), 012066. DOI: https://doi.org/10.1088/1757-899X/737/1/012066
[19] Chen, X., Tang, X., Zhang, C., et al., 2022. Synthesis and property of EPEG -based polycarboxylate ether superplasticizers via RAFT polymerization. Polymer Engineering & Science. 62(9), 2769–2778. DOI: https://doi.org/10.1002/pen.26060
[20] Chen, Z., Chen, B., Tang, Y., et al., 2024. Innovative strategies for time-release PCE design and cement paste flowability control. Cement and Concrete Composites. 154, 105785. DOI: https://doi.org/10.1016/j.cemconcomp.2024.105785
[21] Salih, M.A., Ahmed, S.K., Mohammed, A.S., 2025. Performance of Sustainable Underwater Concrete Containing GGBS and Micro Silica with Anti-Washout. Civil Engineering Journal. 11(12), 5238–5255. DOI: https://doi.org/10.28991/CEJ-2025-011-12-018
[22] Burhan, L., Ghafor, K., Mohammed, A., 2020. Enhancing the Fresh and Hardened Properties of the Early Age Concrete Modified with Powder Polymers and Characterized Using Different Models. Advances in Civil Engineering Materials. 9(1), 227–249. DOI: https://doi.org/10.1520/ACEM20190087
[23] Nili, M., Sabziparvar, N., Sabziparvar, A., 2023. Creep and drying shrinkage of recycled aggregate concrete containing cement and alkali activated slag produced by water reduction method (WRM) and equivalent mortar volume (EMV). Construction and Building Materials. 395, 132153. DOI: https://doi.org/10.1016/j.conbuildmat.2023.132153
[24] ASTM International, 2023. ASTM C230/C230M-23: Standard Specification for Flow Table for Use in Tests of Hydraulic Cement. ASTM International: West Conshohocken, PA, USA. DOI: https://doi.org/10.1520/C0230_C0230M-23
[25] ASTM International, 2026. ASTM C232/C232M-26: Standard Test Method for Bleeding of Concrete. ASTM International: West Conshohocken, PA, USA. DOI: https://doi.org/10.1520/C0232_C0232M-26
[26] U.S. Army Engineer Waterways Experiment Station (WES), 1989. CRD C61–89A: TTest Method for Determining the Resistance of Freshly-Mixed Concrete to Washing Out in Water. U.S. Army Engineer Waterways Experiment Station (WES): Vicksburg, MI, USA. pp 1–3.
[27] ASTM International, 2023. ASTM C403/C403M-23: Standard Test Method for Time of Setting of Concrete Mixtures by Penetration Resistance. ASTM International: West Conshohocken, PA, USA. DOI: https://doi.org/10.1520/C0403_C0403M-23
[28] ASTM International, 2026. ASTM C109/C109M-26: Standard Test Method for Compressive Strength of Hydraulic Cement Mortars (Using 50 mm [2 in.] Cube Specimens). ASTM International: West Conshohocken, PA, USA. DOI: https://doi.org/10.1520/C0109_C0109M-26
[29] Hwalla, J., Saba, M., Assaad, J.J., 2020. Suitability of metakaolin-based geopolymers for underwater applications. Materials and Structures. 53(5), 119. DOI: https://doi.org/10.1617/s11527-020-01546-0
[30] Zhuang, S., Wang, Q., Zhang, M., 2022. Water absorption behaviour of concrete: Novel experimental findings and model characterization. Journal of Building Engineering. 53, 104602. DOI: https://doi.org/10.1016/j.jobe.2022.104602
[31] Kabir, H., Garg, N., 2023. Rapid prediction of cementitious initial sorptivity via surface wettability. npj Materials Degradation. 7(1), 52. DOI: https://doi.org/10.1038/s41529-023-00371-4
[32] Belal, M.H., Heniegal, A.M., Ragheb, S.R., et al., 2026. Enhancing washout resistance and durability of slag-based underwater concrete incorporating eco-friendly ternary binders and recycled aggregates. Construction and Building Materials. 531, 146675. DOI: https://doi.org/10.1016/j.conbuild-

mat.2026.146675

[33] Li, L.G., Zhang, G.-H., 2024. Feasibility of underwater 3D printing: Effects of anti-washout admixtures on printability and strength of mortar. Journal of Building Engineering. 96, 110434. DOI: https://doi.org/10.1016/j.jobe.2024.110434

[34] Chen, W., Zhou, Y., Yu, Q., et al., 2024. Microscopic thickening mechanisms of hydroxypropyl methyl cellulose ether anti-washout admixture and its impact on cementitious material rheology and anti-dispersal performance. Journal of Building Engineering. 89, 109346. DOI: https://doi.org/10.1016/j.jobe.2024.109346

[35] Nia, S.B., Shafei, B., 2026. Advances in underwater concrete mixtures: Correlation of anti-washout requirements with rheological, mechanical, and durability properties. Results in Engineering. 31, 111439. DOI: https://doi.org/10.1016/j.rineng.2026.111439

[36] Guo, Y., Zhou, Z., Ma, A., et al., 2026. Phase separation and gelation behavior of the mixtures of welan gum and pea protein. Food Hydrocolloids. 171, 111774. DOI: https://doi.org/10.1016/j.foodhyd.2025.111774

[37] Tian, C., Chen, N., Su, Y., et al., 2024. Rheological properties and shrinkage crack resistance of welan gum-modified cementitious materials. Construction and Building Materials. 441, 137539. DOI: https://doi.org/10.1016/j.conbuildmat.2024.137539